

Chapter Number

Applicability of GFP Microbial Whole Cell Biosensors to Bioreactor Operations - Mathematical Modeling and Related Experimental Tools

Delvigne Frank¹, Brognaux Alison¹, Gorret Nathalie²,
Sørensen J. Søren³, Crine Michel⁴ and Thonart Philippe¹

¹ *Université de Liège, Gembloux Agro-Bio Tech, Unité de Bio-industries/CWBI**

² *Université de Toulouse, INSA, INRA, UMR792*

Ingénierie des Systèmes Biologiques et Procédés

³ *University of Copenhagen, Department of microbiology, Søløgade 83H, 1307 Copenhagen*

⁴ *Université de Liège, Chemical engineering laboratory*

^{1,4}*Belgium*

²*France*

³*Denmark*

1. Introduction

Until now, whole cell microbial biosensors have been mainly used for the detection of chemicals in different ecosystems (Sorensen, 2006). In this work, we propose to point out different features of microbial biosensors in the context of their applicability to monitor bioreactor operations. Indeed, large-scale bioreactors tend to be heterogeneous and it is now clear that these heterogeneities (e.g. in substrate, dissolved oxygen, pH, temperature,...) induce several kinds of physiological responses at the level of the exposed microbial cells, i.e., metabolic shift (Xu, 1999, Neubauer, 1995, Han L., 2002), mRNA synthesis (Schweder, 1999), stress protein synthesis (Schweder, 2004, Pioch, 2007), alteration of membrane integrity (Hewitt, 2000, Nebe-von-Caron G., 2000). In this context, the use of Green Fluorescent Protein (GFP) microbial whole cell biosensors is fully justified by their recognized advantages: characterization of the physico-chemical conditions at the micrometer scale when analyzed at the single cell level (Tecon, 2006, Southward, 2002), non-invasive measurement and possibility to acquire online signal (Jones, 2004). Two main problems are encountered when extending the use of microbial biosensors for monitoring bioreactor efficiency, i.e. first the choice of an appropriate stress promoter for the detection of extracellular fluctuations and second the dynamics of the expression of the reporter system in front of the bioreactors hydrodynamics. This last issue is especially critical considering the particular dynamics of extracellular fluctuations encountered in the reacting volume depending on bioreactor mixing efficiency, circulation of microbial cells inside the

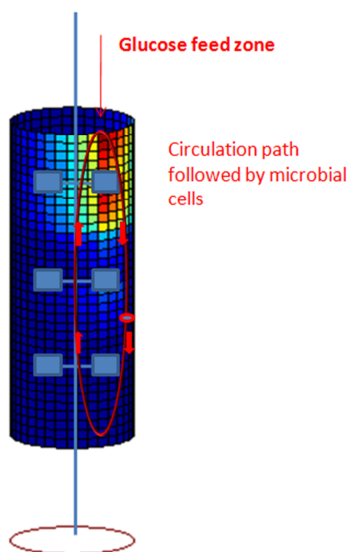
* Corresponding author: F.Delvigne@ulg.ac.be

1 broth and the dynamics of substrate consumption. Discussion will be supported by
2 mathematical simulations of the dynamics of GFP expression inside microbial biosensors
3 and of the bioreactor hydrodynamics.

4 **2. Basic microbial biosensor design and its application to bioreactor** 5 **operations**

6 **2.1 Basic bioreactor design : the scaling-up problematic and the potential role of** 7 **microbial biosensors**

8 The main problem associated with bioprocesses scaling-up is the formation of concentration
9 gradients inside large-scale bioreactors (Hewitt, 2007a, Lara, 2006, Enfors, 2001). These
10 gradients induce various stresses at the level of microbial cells, such as glucose excess, glucose
11 starvation, oxygen limitation, pH shock, leading to a deviation of the cells from the desired
12 metabolism and in extreme case to a complete modification of the metabolism subsequent to a
13 modification of the gene expression pattern. Studies have been mainly focused on glucose
14 gradient appearing during fed-batch process, although other kinds of gradient have also been
15 considered (Neubauer, 2010). The characterization of the exposure of microorganisms to
16 gradients stress is not a trivial task, since several phenomena, including bioreactor mixing
17 efficiency and microorganism's circulation, are involved (Fig. 1).
18



19
20 Fig. 1. Illustration of the exposure of microbial cells to glucose gradient concentration inside
21 an industrial bioreactor operating in fed-batch mode. The color intensity is proportional to
22 the glucose concentration and the figure shows that glucose accumulates at the level of the
23 upper part of the bioreactor considering the lack at the level of the mixing efficiency of the
24 system

25 Actually, because of the lack of appropriate sensors, bioprocess monitoring rely on indirect,
26 global parameters, such as biomass evolution, substrate uptake profile, and these

1 parameters are not directly related to the cells physiological state (Deckwer, 2006, Pioch,
2 2007, Clementschitsch F., 2006). As reported in previous studies, stress genes can be used as
3 marker in order to monitor the fitness of bacterial systems during industrial bioprocesses
4 (Schweder, 2004). We propose thus to use several stress promoters linked with the GFP
5 doing sequence and inserted in microbial cells in order to design some kind of
6 "physiological tracer" for the determination of the biological impact of the mixing conditions
7 met in heterogeneous bioreactors. These analyses will be performed by considering several
8 *E. coli* strains carrying a Green Fluorescent Protein (GFP) reporter system. This kind of
9 reporter system provides rapid detection of the promoter expression level (March, 2003), at
10 a single cell level (by using flow cytometry) and by taking the population dynamics into
11 account (Patkar, 2002). Indeed, previous studies have shown that microbial population can
12 be very heterogeneous in a bioreactor, according to a particular cellular function (Hewitt,
13 2007b, Sundstrom, 2004, Roostalu, 2008). It is why a large part of this work will be devoted to
14 the demonstration of the usefulness of GFP reporter strains combined with a flow cytometry
15 analytical tool in order to characterize the stress experienced by microorganisms in perturbed
16 fed-batch bioreactors. As said before, this combination of biological and analytical techniques
17 allows the observation of the consequences of stress at a single cell resolution among a
18 microbial population. By comparison with inert tracer experiments used to characterize
19 bioreactor hydrodynamics, the GFP reporter system takes into account the cell history, i.e. the
20 displacement of the microbial particle along the concentration gradient. This reporter system is
21 also linked with a direct physiological parameter, i.e. the protein synthesis related to an
22 extracellular stimulus. It must be noted that, although protein synthesis is the final
23 consequence of a physiological reaction (e.g., synthesis of a stress protein that redirect
24 metabolic activity to better cope with stress conditions), the characteristic time constant
25 associated with this biological reaction is rather high compared with circulation and mixing
26 time inside bioreactors. The major challenge of this work is thus to demonstrate that useful
27 information can be gained from the analysis of the GFP microbial biosensor dynamics after the
28 response of the microbial population to various process-related perturbations.

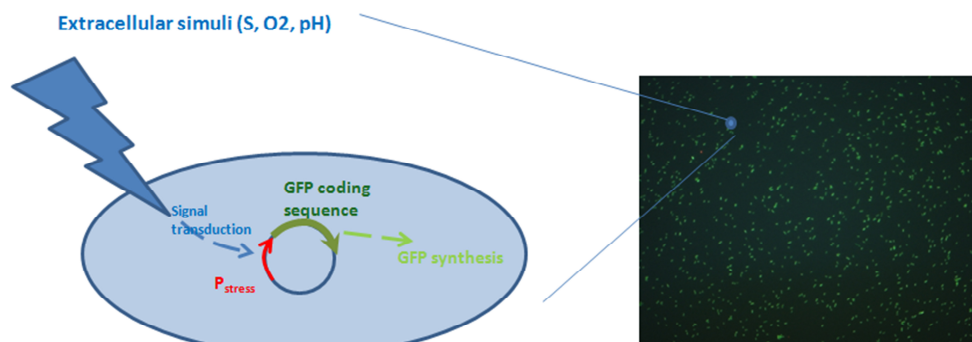
29 **2.2 Selection of an appropriate stress promoter**

30 The critical step for an appropriate biosensor design, apart from the characteristics of the
31 GFP itself, relies on the choice of a stress promoter. This is this part of the biosensor that will
32 be sensitive to the extracellular conditions met by microbial cells inside bioreactors (Fig. 2).

33 According to their specificity, three classes of promoter can be considered in order to build
34 the reporter system (Sorensen, 2006):

- 35 - Non-specific: the reporter gene coding for GFP is linked to a constitutive promoter. This
36 kind of construction has been previously used to toxicants in various environments
37 (Wiles, 2003, Bhattacharyy, 2005). Since the promoter is constitutively expressed, cells
38 that are exposed to lethal dose of toxicants do not exhibit any fluorescence and can be
39 easily distinguished from not exposed biosensors. Owing to their simplicity, non-
40 specific reporters are the most widely used whole-cell biosensors.
- 41 - Semi-specific: the reporter gene is linked with a promoter responding to general
42 conditions of stress. In this case, the biosensor is activated when cells are exposed to
43 stressful conditions. Stress promoters can be selected on the basis of their belonging to
44 well-known stress regulon, such as the heat shock or the general stress response
45 regulons (e.g., *rpoS* regulon for several Gram negative bacteria, including *E. coli*).

- 1 - Specific: the biosensor specifically responds to the presence of a defined chemical. It
 2 implies the selection of a promoter that is tightly regulated by the presence of a specific
 3 chemical signal.
 4



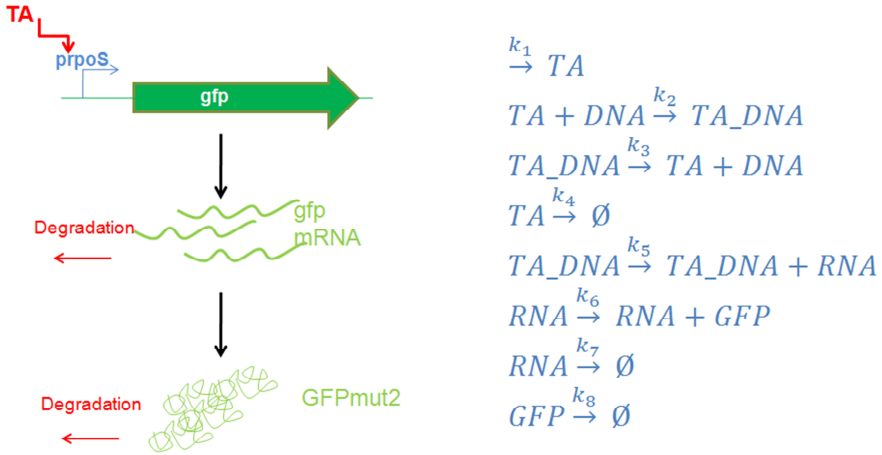
5
 6 Fig. 2. Basic principle of GFP microbial biosensors. Photograph on the right shows the
 7 process of GFP synthesis inside *E. coli* biosensors

8 In bioreactor, the environment detected by the cells comprises multiple variables, such as
 9 substrate level, pH, dissolved oxygen and temperature. The use of specific biosensor is thus
 10 not adapted in bioreactor applications, although some studies involve the use of such
 11 system (e.g., the use of the *narZ* promoter coupled to the GFP coding sequence in order to
 12 detect local oxygen limitation in bioreactors (Garcia, 2009)). It must also point out that the
 13 reporter system governs the field of application of the considered microbial biosensor.
 14 Indeed, if GFP is used as signaling system, only aerobic processes can be investigated,
 15 considering that maturation of the GFP molecule requires an oxidation step promoted by
 16 the presence of oxygen in the medium (Tsien R.Y., 1998). In our case, we will select stress
 17 promoter responsive to carbon limitation. This stimulus is in fact mainly encountered in
 18 intensive fed-batch operation, one of the most used modes of operation at the industrial
 19 level considering its enhanced productivity. Then, in normal fed-batch mode it is expected
 20 that the microbial biosensor is fully activated and exhibit a given level of fluorescence
 21 according to the strength of the associated stress promoter, and when biosensor is exposed
 22 to deviation from the normal feeding profile, GFP level decreases. These considerations
 23 about the performances of fed-batch bioreactor will be explained more in details in section 4.

24 **2.3 Dynamics of the microbial biosensor and method for GFP detection**

25 When the appropriate stress promoter has been selected, the characteristic of the reporter
 26 molecule itself, i.e. GFP, must be kept into account. Indeed, GFP synthesis depends on a
 27 huge amount of factors, such as plasmid copy number (if the reporter system is carried by a
 28 plasmid), promoter strength, but also the rate of transcription and translation and the half-
 29 life of the GFP mRNA and proteins. One of the major drawbacks associated with the first
 30 version of GFP used as reporter system was its folding and maturation time of about 95
 31 minutes (DeLisa, 1999), limiting the use of GFP to characterize the dynamics of microbial
 32 process in bioreactor. Until this, intensive researches have been provided in order to find
 33 out GFP variant of different colors (Shaner, 2005) and exhibiting significantly reduced

1 maturation time (Cormack, 2000). This has led to the GFPmut1, 2 and 3 variants with
2 maturation of about 4 minutes. Another issue was the high stability of this variant. In fact,
3 the stability of the *gfpmut2* variant is so high that this protein exhibits half-life of more than
4 24 hours. In order to illustrate the previous statement, a model allowing the simulation of
5 GFP synthesis has been set up. This model is partly inspired from (Thattai M., 2004) and
6 take into account the essential step involved in GFP expression (Fig. 3).
7



8
9 Fig. 3. Scheme showing the different steps involved for GFP synthesis and related chemical
10 reactions with specific rates (from k_1 to k_8)

11 In our case, synthesis of transcription activator (TA) will depend on the exposure of
12 microbial cells to heterogeneous conditions at the level of the bioreactor (Fig. 3). When TA is
13 synthesized, it binds to the stress promoter (here, *rpoS* promoter has been chosen as an
14 example) and the TA-DNA complex induces a cascade of reactions involving transcription
15 of GFP-related mRNA and translation of this RNA to actively fluorescent GFP.
16 In this work, the *gfpmut2* variant will be used (details about GFP biosensors will be given in
17 section 3). The dynamics of our microbial biosensors will be experimentally characterized in
18 section 4. The dynamics of this set of reactions can be mathematically modeled by 5 ordinary
19 differential equations (ODEs) involving synthesis and degradation of the different chemicals
20 involved (i.e. TA, TA-DNA, DNA, RNA and GFP):

$$21 \quad \frac{dTA}{dt} = k_1 - k_2 \cdot TA \cdot DNA - k_4 \cdot TA + k_3 \cdot TA_DNA \quad (1)$$

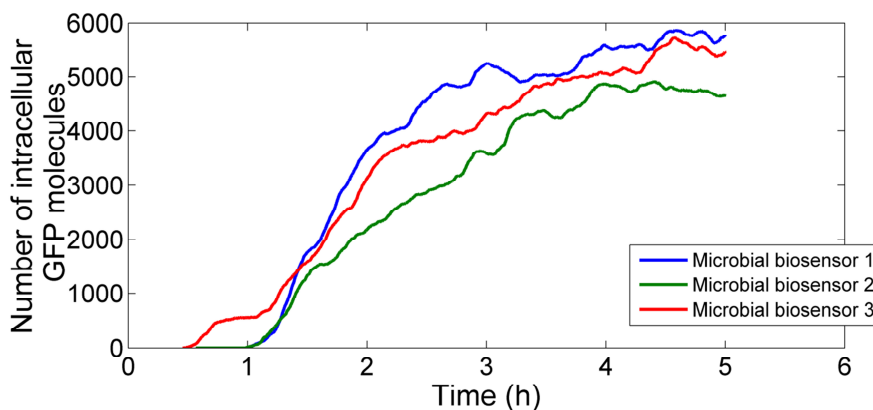
$$22 \quad \frac{dTA_DNA}{dt} = k_2 \cdot TA \cdot DNA - k_5 \cdot TA_DNA - k_3 \cdot TA_DNA \quad (2)$$

$$23 \quad \frac{dDNA}{dt} = k_3 \cdot TA_DNA - k_2 \cdot TA \cdot DNA \quad (3)$$

$$24 \quad \frac{dRNA}{dt} = k_5 \cdot TA_DNA - k_6 \cdot RNA - k_7 \cdot RNA \quad (4)$$

$$25 \quad \frac{dGFP}{dt} = k_6 \cdot RNA - k_8 \cdot GFP \quad (5)$$

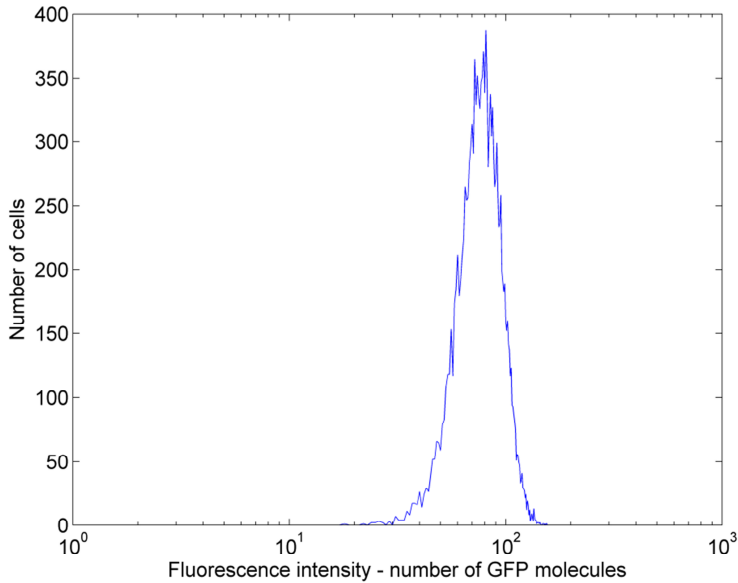
1 These equations can be used in order to predict the time required to reach a given GFP
2 expression level after gene induction. Basically, GFP-related fluorescence can be monitored
3 non-invasively and in a non-destructive way by a lot of equipments comprising excitation
4 sources and appropriate photomultipliers (Randers-Eichhorn, 1997, Kostov, 2000). However,
5 there are more and more GFP measurements carried out with flow cytometer (Patkar, 2002,
6 Galbraith, 1999, Tracy, 2010, Diaz, 2010). This equipment allows the separation of cells prior
7 to analysis, leading to single-cell measurements. The major reason for this increasing interest
8 for flow cytometry relies on the fact that microbial cells are able to exhibit various
9 phenotypes in a same culture broth. Many reasons have been identified to lead to this
10 phenotypic heterogeneity, among which various intrinsic biological processes (cell cycle and
11 division) and extrinsic physico-chemical conditions (impact of the environment on microbial
12 cells) (Müller, 2010). In our case, the recognized stochasticity associated to gene expression
13 (MacAdams H.H., 1997, Swain P.S., 2002) is of major importance since it affects directly GFP
14 synthesis (Mettetal, 2006). To account for these random components, several stochastic
15 models have been developed. Most of these modes are based on the Gillespie algorithm in
16 order to include the stochasticity at the level of the biochemical reactions (Gillespie D.T.,
17 2001). In order to demonstrate the potential impact of stochastic gene expression on GFP
18 synthesis, equations (1) to (5) have been implemented at the level of the Gillespie algorithm.
19 Simulation has been performed with the following parameters: $k_1 = 0.1 \text{ s}^{-1}$; $k_2 = 0.05 \text{ s}^{-1}$; $k_3 =$
20 0.045 s^{-1} ; $k_4 = 0.09 \text{ s}^{-1}$; $k_5 = 0.1 \text{ s}^{-1}$; $k_7 = 0.0058 \text{ s}^{-1}$; $k_6 = 0.1155 \text{ s}^{-1}$; $k_8 = 0.0002 \text{ s}^{-1}$, and considers
21 that the biosensor is activated after 1hour (Fig. 4). Simulated results show that GFP content
22 at the single cell level can vary according to the random nature of the biochemical reactions
23 (Fig. 3). This randomness has to be attributed to the extremely small reacting volume
24 represented by the microbial envelope and the rather small amount of DNA and RNA
25 molecules involved.
26



27
28 Fig. 4. Stochastic simulation of the GFP evolution at the single cell level according to the
29 biochemical reaction scheme depicted at figure 3.

30 By repeating several time the simulation, it is possible to simulate the fate of GFP expression
31 at the single cell level for a whole microbial population. By this way, phenotypic
32 heterogeneity can be taken into account. Comparison with experimental results obtained by

1 flow cytometry is also possible by taking into account the background noise and the
2 sensitivity of this equipment (Zhang, 2006) (Fig. 5).
3



4
5 Fig. 5. Simulated histogram for the GFP content at the single cell level for a given time
6 during bioreactor cultivation

7 The purpose of this work is to demonstrate the applicability for the use of microbial
8 biosensor in a fluctuating reacting volume representative of that encountered in large-scale
9 bioreactor. Single cell behavior will be investigated in order to highlight the impact of both
10 intrinsic and extrinsic sources of noise at the level of GFP expression.

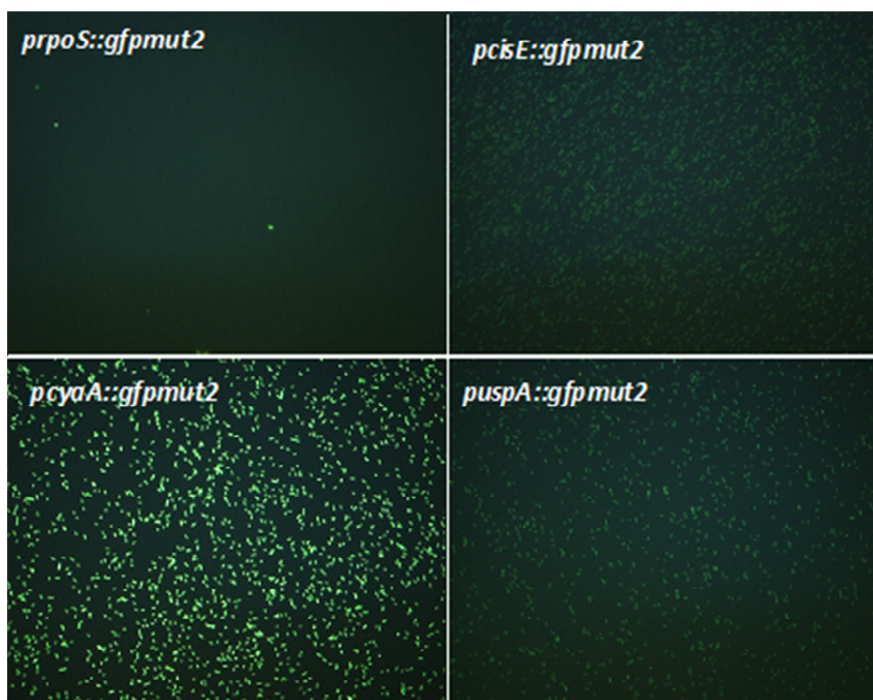
11 **3. "Material and methods" items used in order to illustrate the principles** 12 **covered in this chapter**

13 The experimental results that will be used to illustrate this chapter come from an important
14 set of experiments involving different *E. coli* GFP reporter strains coming from a public
15 collection (Zaslaver, 2006). Two techniques have been used for GFP detection: a classical
16 spectrofluorimeter and flow cytometry. Most of the experiments carried out in this work
17 have been based on a fluorescence signal are measured by flow cytometry, considering the
18 single cell capability of this techniques. This approach allows to interpret the data by
19 considering the stochastic mechanisms (noise) inherent to GFP expression and to
20 fluctuations met in heterogeneous environment (Müller, 2010, Patnaik, 2002, Patnaik P.R.,
21 2006). Techniques are detailed in the following sections.

22 **3.1 Strains and medium**

23 *E. coli* K12 MG1655 bearing a pMS201 (4260 bp) plasmid with a stress promoter and a
24 kanamycin resistance gene. The strains comes from a cloning vector library elaborated at the

1 Weizmann Institute of Science (Zaslaver, 2006). Three reporter strains have been selected
2 from this library, according to the responsiveness of their promoter to carbon limitation, i.e.
3 the general stress response promoter *rpoS*, the carbon starvation induced promoter *csiE* and
4 the universal stress protein associated promoter *uspA*. A constitutive promoter *cyaA* has
5 been used as a basis for comparison (Fig. 6). Microbial biosensors are maintained at -80°C in
6 working seeds vials (2 mL) in solution with LB media and with 40% of glycerol. Precultures
7 and cultures have been performed on a defined mineral salt medium containing (in g/L):
8 K_2HPO_4 14.6, $NaH_2PO_4 \cdot 2H_2O$ 3.6 ; Na_2SO_4 2 ; $(NH_4)_2SO_4$ 2.47, NH_4Cl 0.5, $(NH_4)_2$ -H-citrate
9 1, glucose 5, thiamine 0.01, kanamycin 0.1. Thiamin and kanamycin are sterilized by
10 filtration (0.2 μ m). The medium is supplemented with 3mL/L of trace solution, 3mL/L of
11 a $FeCl_3 \cdot 6H_2O$ solution (16.7 g/L), 3mL/L of an EDTA solution (20.1 g/L) and 2mL/L of a
12 $MgSO_4$ solution (120 g/L). The trace solution contains (in g/L): $CoCl_2 \cdot H_2O$ 0.74,
13 $ZnSO_4 \cdot 7H_2O$ 0.18, $MnSO_4 \cdot H_2O$ 0.1, $CuSO_4 \cdot 5H_2O$, $CoSO_4 \cdot 7H_2O$. Before each bioreactor
14 cultivation experiment, a precultivation step is performed in 100 mL of the above
15 mentioned medium in baffled shake flask at 37°C and under orbital shaking at 160 rounds
16 per minute. Cell growth has been monitored by optical density (OD) at a wavelength of
17 600 nm. Cell dry weight has been determined on the basis of filtered samples (0.45 μ m)
18 dried during 24 hours at 105°C. Glucose concentration has been monitored by an electro-
19 enzymatic system YSI.
20



21
22 Fig. 6. Epifluorescence microscopy pictures showing the relative intensity of the basal level
23 of GFP expression for the different microbial biosensors involved in this work

3.2 Bioreactor configurations

Microbial GFP biosensors have been cultivated in a lab-scale stirred bioreactors (Biostat B-Twin, Sartorius) operated in fed-batch mode (total volume: 3L; initial working volume: 1L; final working volume: 1.5L; mixing provided by a standard RTD6 rushton turbine). The bioreactor platform comprises 2 cultivation vessels in parallel monitored and controlled by the same control unit (remote control by the MFCS/win 3.0 software). For each reporter strains, experiments have been conducted in parallel by considering a culture performed in the classical stirred vessel and another one conducted with the stirred vessel connected to a recycle loop. This last apparatus correspond to a scale-down strategy allowing to reproduce heterogeneities expected in large-scale bioreactors (Hewitt, 2007a, Lara, 2006, Delvigne, 2006a). The scale-down reactor arrangement is based on the previously described stirred bioreactor connected to a recycle loop (silicon pipe; diameter 0.005m ; length 6m or 12m in order to modulate the residence time in the recycle loop). A continuous recirculation of the broth between the stirred reactor and the recycle loop is ensured by a peristaltic pump (Watson Marlow 323) with the glucose feed solution being added at the inlet of the recycle loop in order to generate a concentration gradient. Fed-batch is controlled on the basis of dissolved oxygen (setpoint : 30% above saturation). The dissolved oxygen in the recycle loop is monitored by a set of sterilizable optical probes (Flow-through cell, Presens). The sensor spot inserted in the flow-through cell contains a fluorogenic compound that is excited at a wavelength of 540 nm. The emission signal can then be recorded at 640 nm. The dissolved oxygen measurement is based on the properties that molecular oxygen is able to absorb a part of the emission energy. The relationship between dissolved oxygen and fluorescence intensity is nonlinear and can be expressed by the Stern-Volmer equation (John, 2003). The excitation and emission signals are generated / recorded at the level of a miniaturized set of excitation led and photomultiplier. The fluorescence signal coming from planar sensors is then processed and recorded at the level of an oxy-4 mini transmitter. During the experiments, pH was maintained at 6.9 (regulation by ammonia and phosphoric acid) and temperature at 37°C. Stirrer rate is maintained at 1000 rpm with a RDT6 impeller and air flow rate is set to 1 L/min at the beginning of the culture. When fed-batch is started agitation rate and air flow rate are progressively raised to 1300 rpm and 2 L/min respectively. Culture is fed with 500 mL of a solution containing 400 g/L of glucose diluted in mineral medium (see above for composition). Continuous cultures have also been performed on the basis of the same stirred bioreactor with the same settings. In this case, fresh culture medium is added continuously and spent medium is withdrawn in order to keep a constant volume. The fresh medium feed rate is modulated in order to reach dilution rate of 0.02 h⁻¹ and 0.2 h⁻¹.

3.3 Flow cytometry

The analysis of the GFP expression level has been performed by Fluorescence Activated Cell Sorting (FACS) on a FACScan (Becton Dickinson) flow cytometer. Samples are taken directly from the reactor and are diluted in 900 µL of PBS and 100 µL of a chloramphenicol solution (50 µg/mL) in order to stop protein synthesis. For each measurement, 30,000 cells are analyzed. GFP is excited at 488 nm and emission signals are collected by using filters at 530 nm. The gfp-mut2 variant has been especially engineered to optimally match the excitation/emission range of the FACS instrument (Cormack, 1996). Considering that bacterial cells exhibit a high side scatter (SSC) signal (Galbraith, 1999), a threshold of 52 has been set up on the SSC channel in order to limit noise signal. The FSC, FL1, FL2 and FL3

1 channels are logarithmically amplified with the following settings: FSC E00, FL1 620, FL2
 2 420, FL3 420. The results have been analyzed by the FlowJo version 7.6.1 software. Flow
 3 cytometry has also been used in order to determine the residence time distribution inside
 4 the recycle loop of the SDRs and the membrane permeability of the cells (see above).

5 **3.4 Tracer test for the determination of the residence time distribution inside the** 6 **recycle loop of the SDRs**

7 Fluorescent microspheres (fluorosphere 1 μ m, molecular probes, invitrogen) have been
 8 used as representative tracer for the determination of the residence time distribution of
 9 the microbial cells inside the recycle loop of the SDRs. Indeed, tracer test involving
 10 particulate dye instead of soluble dye has been recently recognized as more relevant to
 11 describe the transport of microbial cells (Asraf-Snir, 2011). We have also use this method
 12 previously for the characterization of the transport of fluorescently labeled microbial cells
 13 in scale-down reactors (Delvigne, 2006b). Our methodology has been improved in the
 14 present work, mainly at the level of the method used to detect fluorescent particles. A
 15 tracer pulse of 1 mL containing 10⁹ fluorescent beads has been injected at the inlet of the
 16 recycle loop. Samples of 3 mL are taken at different time intervals at the outlet of the
 17 recycle loop. Samples are analyzed by flow cytometry. Beads are easily detected according
 18 to their high green fluorescent level (FL1 detection). The analysis is performed for 30s
 19 and the number of events recorded during this period is used as a measure of the beads
 20 concentration. The number of events is gated on the basis of the FL1 parameter in order to
 21 make the distinction between fluorescent beads and background (software analysis
 22 performed on FlowJo 7.6.1.). The RTD curves are processed with MatLab to determine the
 23 following parameters:

$$24 \quad t_R = \frac{\sum_i^{n-i} t_i \cdot C_i \cdot \Delta t_i}{\sum_i^{n-i} C_i \cdot \Delta t_i} \quad (6)$$

$$25 \quad \sigma^2 = \frac{\sum_i^{n-i} t_i^2 \cdot C_i \cdot \Delta t_i}{\sum_i^{n-i} C_i \cdot \Delta t_i} - t_R^2 \quad (7)$$

26 With t_R being the mean residence time of the RTD (s); C_i the number of beads detected
 27 during the time interval t_i and σ^2 the variance of the RTD (s^2).

28 The SDRs considered here comprise a well-mixed stirred bioreactor connected to a recycle
 29 loop. Glucose is injected at the inlet of the recycle loop in order to generate a concentration
 30 gradient. As stated in a previous work, the intensity of the concentration gradient, but also
 31 the frequency at which microbial cells are exposed to these gradients is important (Delvigne,
 32 2006a). In order to assess the performances of the SDRs, the residence time distribution
 33 (RTD) of microbial cells has been determined by using an innovative tracer test.
 34 Mathematical treatment of the RTD curves led to the following results: in the case of the
 35 SDR with a recycle loop $L = 6$ m : mean residence time $t_R = 38.2$ s and variance σ^2 of 62.2 s^2 ;
 36 in the case of the SDR with a recycle loop $L = 12$ m : $t_R = 79.8$ s and $\sigma^2 = 120.7$ s^2 .

37 **3.5 Supernatant analysis: fluorescence, SDS-page and western blot**

38 Samples coming from bioreactor are centrifugated at 12000 rpm for 3 minutes and filtered
 39 on 0.2 μ m cellulose membrane in order to remove the cells. Fluorescence of the supernatant
 40 (samples of 200 μ L on 96 wells black microtiter plate) is analysed by spectrofluorimetry
 41 (Victor³ V Wallac, Perkin Elmer). Proteins coming from the supernatant (7 μ L) are separated

1 on 30% polyacrylamide gels (Biorad). Immunoblot is performed in order to detect the band
2 corresponding to GFP (ECL plus detection system, Amersham).

3 **3.6 Membrane permeability**

4 Samples taken from bioreactor are diluted in PBS in order to reach an optical density of 4.
5 Cells are stained by adding 10 μ L of propidium iodide solution (PI) for 15 minutes at 37°C.
6 Samples are then analyzed by flow cytometry with the following settings : FSC E00, FL1 620,
7 FL2 420, FL3 520.

8 **3.7 Mathematical modeling**

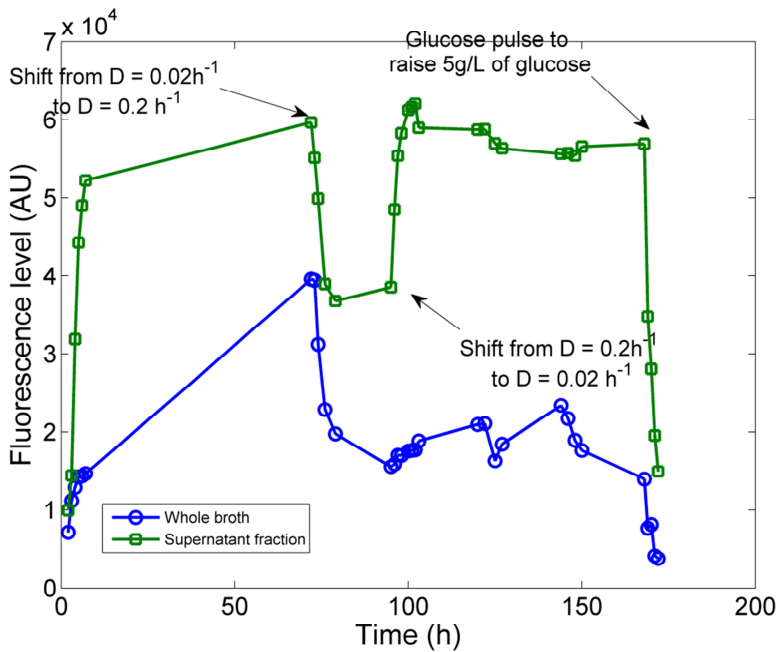
9 Mathematical modeling procedures allowing the simulation of the gradients experienced by
10 microbial biosensors developed in this work will be explained directly in the text for the
11 ease of understanding. All the codes are written in MatLab and are based on standard
12 algorithm (notably the ode function has been used for the resolution of ODEs systems).
13 Sample codes are provided in annex. Please refer to a reference book (e.g., (Finlayson, 2006))
14 for additional explanations about appropriate use of the .m codes.

15 **4. Investigation of the dynamics of several GFP microbial biosensors** 16 **responsive to substrate limitation**

17 Two strategies, involving each a given bioreactor mode of operation, will be considered in
18 order to assess the performance of selected microbial biosensors. The chemostat reactor
19 allows to test the responsiveness of the microbial biosensor in fully stabilized conditions,
20 whereas the scale-down reactor (SDR) allows to better reproduce the complex
21 environmental perturbations encountered in industrial scale bioreactor operating in fed-
22 batch mode.

23 **4.1 Investigation in continuous bioreactors : chemostat mode**

24 In order to assess the responsiveness of the microbial biosensor, a culture in chemostat
25 mode has been performed by considering a sharp variation at the level of the dilution rate.
26 Indeed, the *csiE* biosensor is supposed to be induced upon carbon limitation, a condition
27 that can be easily implemented in a chemostat under controlled conditions (i.e., constant cell
28 density and growth rate with constant environmental variables such as pH and dissolved
29 oxygen). The culture is started by a batch phase and no evolution of the fluorescence is
30 noticed during this phase according to the fact that microbial growth is not limited and
31 substrate is in large excess. At the end of the batch phase, bioreactor is switched to
32 continuous mode at a very low dilution rate of 0.02 h⁻¹ (Fig. 7) At this stage, *csiE* promoter is
33 activated and fluorescence level rises significantly and reach a constant value after 60 hours
34 of culture (corresponding to the equilibrium time considered when using a D = 0.02 h⁻¹).
35 When equilibrium is reached, dilution rate is rapidly switched to 0.2 h⁻¹ leading to a shift of
36 the environmental conditions to less limiting at the level of the carbon source. As expected,
37 fluorescence level drops considering the decrease of the activation of the *csiE* promoter.
38 However, fluorescence level does not go back to its initial basal level. As a last step of
39 experiment, a glucose pulse of 5 g/L has been performed in order to relieve completely
40 glucose limitation leading to the drop of fluorescence level to its initial state. This series of
41 experiments validate the responsiveness of the *csiE* promoter to glucose limitation.

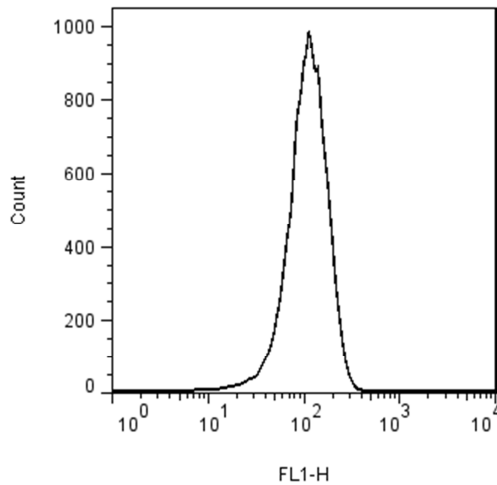


1
2 Fig. 7. Evolution of the global fluorescence for a culture carried out by using the *csiE*
3 microbial biosensor in chemostat. Initial batch phase ends at 2 hours and is followed by a
4 continuous mode of culture.

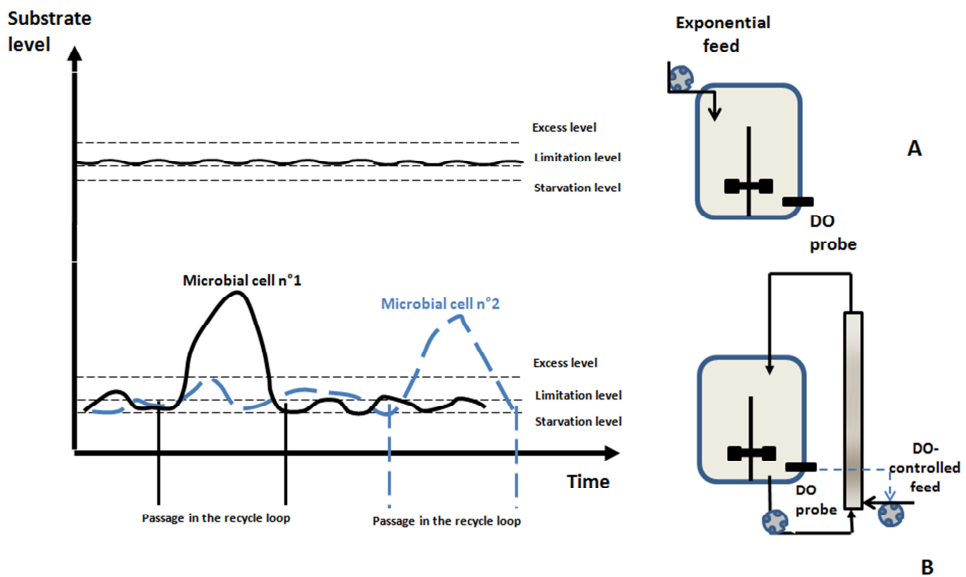
5 The GFP distribution among the microbial population has been determined by flow
6 cytometry (Fig. 8). Results show that, even when all the microbial biosensors are cultivated
7 under strictly constant environmental conditions, heterogeneity at the level expression is
8 observed. This phenomenon has to be attributed to the stochastic mechanisms governing
9 GFP expression (described as the intrinsic source of noise in section 2) and must be further
10 taken into account to make the difference between intrinsic and extrinsic or environmental
11 source of noise. The extrinsic source of noise will be experimentally generated at the level of
12 a scale-down bioreactor.

13 4.2 Investigation in scale-down reactors (SDR)

14 In industrial bioreactor, the picture is by far more complex since extrinsic noise has to be
15 added to the intrinsic one. Indeed, the drop of mixing efficiency induces the appearance of
16 concentration gradient. In order to characterize the concentration fluctuations met by the
17 microbial cells, the circulation process must be superimposed to the concentration gradient.
18 However, it is well known that this circulation process is subject to stochasticity in large-
19 scale bioreactor, and can be characterized by a circulation time distribution (Nienow A.W.,
20 1998). This kind of stochastic process is at the basis of the extrinsic source of noise, i.e. the
21 extracellular fluctuations experienced by the cells and potentially leading to a stress
22 response (Müller, 2010). In order to take into account this extrinsic component, a two-
23 compartment scale-down bioreactor experiment has been set up. In this kind of apparatus,
24 the passage of the cells through the tubular section is an extrinsic stochastic phenomenon

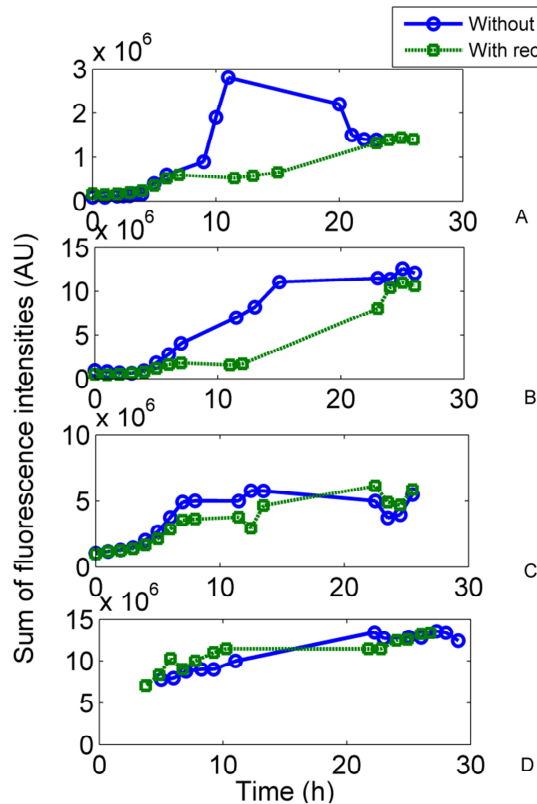


1
 2 Fig. 8. Distribution of the GFP-related fluorescence determined by flow cytometry (green
 3 component of the fluorescence determined by the FL1 channel). Sample has been taken from
 4 a culture involving the *csiE* biosensor in a chemostat at $D = 0.02 \text{ h}^{-1}$
 5 that leads to the exposure to local glucose fluctuations. By this way, it is possible to expose
 6 the microbial cells belonging to the same population to extracellular fluctuations at different
 7 frequencies and intensities (Fig. 9).
 8



9
 10 Fig. 9. Illustration of the scale-down reactor (B) principle and comparison with normal (A)
 11 mode of substrate addition during fed-batch

1 The dynamics of four GFP biosensors have been tested comparatively in a stirred bioreactor
 2 (considered as well-mixed) and a scale-down reactor with a recycle loop (Fig. 10).
 3



4
 5 Fig. 10. Evolution of the GFP-related fluorescence for the *rpoS* (A), *csiE* (B), *uspA* (C) and
 6 *cyaA* (D) biosensor in lab-scale bioreactor and in SDR

7 The *cyaA* strain has been chosen as a reference and exhibits a strong constitutive GFP
 8 expression throughout the culture. In addition, GFP expression is not affected by the
 9 perturbations induced by the presence of the recycle loop in the case of the SDR experiment.
 10 For the three other reporter strains involving stress promoters, a significant induction is
 11 observed when the bioreactor is shift to the fed-batch mode after 4 hours of cultivation. The
 12 *rpoS* and *csiE* exhibits a very low basal level of GFP expression, whereas this basal level is
 13 high in the case of the *uspA* strain. This quite high basal level has been previously observed
 14 with an equivalent *lacZ* transcriptional reporter strain cultivated in fed-batch mode (Prytz,
 15 2003). A significant difference has been noticed at the level of the induction profile between
 16 classical and scale-down bioreactor for the *rpoS* and *csiE* strains. This environmental
 17 condition seems to be met during the fed-batch culture when the carbon flow inside the
 18 bioreactor is limited in order to avoid dissolved oxygen limitation. In the case of the scale-
 19 down bioreactor experiments, glucose is injected at the level of the recycle loop and
 20 microbial cells are thus exposed to glucose fluctuations. In our case, these fluctuations tend

1 to slow down the induction dynamics of the promoters associated to the carbon starvation
2 network. The *rpoS* promoter induces the expression of the sigma S factor, i.e. the master
3 regulator of the general stress response when *E. coli* is carbon limited or starved (Storz,
4 2000). Interestingly, the *csiE* promoter is sigma S dependent (Marschall, 1995) and exhibits
5 also a significant difference of level of induction when the corresponding reporter strain is
6 cultivated in SDR. The *uspA* reporter strain shows no significant difference at the level of the
7 GFP intensity when the culture is performed in classical bioreactor or in SDR. In all cases,
8 the three stress promoters (the *cyaA* being considered as constitutive) show a significant
9 increase in their level of induction when cultures are shifted to fed-batch mode. This
10 observation can be attributed to the fact that the *rpoS*, *cisE* and *uspA* promoters are known to
11 be induced in carbon limiting conditions which is the case in our fed-batch experiments. At
12 this stage, it is important to relate biosensor response to environmental perturbations
13 experienced in SDR. This point will be discussed in the next section.

14 **5. Mathematical modelling of the local heterogeneities met by microbial cells** 15 **in scale-down bioreactors**

16 The characterization of the environmental fluctuations perceived by microbial biosensors is
17 an essential step in order to understand the dynamics of GFP expression. However, the
18 extracellular perturbations perceived at the single cell level involve several components
19 including bioreactor hydrodynamics, but also the displacement of the microbial cells
20 themselves along the gradient field. The purpose of the next two sections is to provide the
21 reader with basic and advanced mathematical tools in order to simulate concentration
22 fluctuations perceived at the single cell level in a SDR.

23 **5.1 Simulation of the concentration gradient fields inside bioreactors**

24 The appearance of concentration gradients (substrate, dissolved oxygen, pH,...) in large-
25 scale bioreactors can have severe consequences at the level of the viability of the
26 microorganisms and thus at the level of the bioprocesses performances. The characterization
27 of these gradients in function of the bioreactor design modification and the up-scaling
28 procedures is of particular importance and is generally achieved by the aim of structured
29 hydrodynamic models that can be classified into three distinct classes with increasing level
30 of complexity (Guillard F., 1999). The simplest structured hydrodynamic model is based on
31 a rough compartmentalisation of the bioreactor in a few virtual fluid zones. This kind of
32 model has been used with success to characterize axial concentration gradient in multi-
33 impeller systems (Mayr B., 1993, Vrabel P., 2001, Machon V., 2000, Cui Y.Q., 1996,
34 Vasconcelos J.M.T., 1995). The advantage of such model relies on its simple physical and
35 mathematical representation, i.e. respectively mass balance and ordinary differential
36 equations, for the expression of the time evolution of a given chemical species in each
37 compartment, allowing to connect the hydrodynamic modeling procedure with complex
38 microbial growth model (Vrabel P., 2001). However, the compartment model is limited by
39 its poor spatial resolution. This problem has been overcome by the use of network-of-zones
40 (NOZ) models. The NOZ model is based on the same physical and mathematical principles
41 than for the compartment model, but in this case the number of virtual fluid zones has been
42 significantly increased, allowing a higher spatial discretization of the bioreactor domain.
43 NOZ models comprising up to 36,000 fluid zones have been used (Hristov H.V., 2004) and
44 have allowed to capture to some extent the complex liquid or gas-liquid flow patterns in

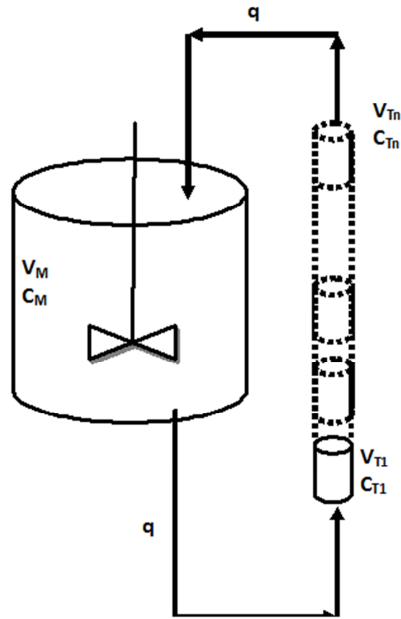
1 stirred or pneumatically agitated bioreactors (Hristov H.V., 2004, Zahradnik J., 2001, Mann
2 R., 1997). However, the elaboration of NOZ models is based on some prior knowledge, such
3 as the streamlines pattern (Hristov H.V., 2004), which is difficult to obtain for complex
4 turbulent flow. A second limitation is the hypothesis that all the circulation flows between
5 the fluid zones have the same intensities, which can lead to the abstraction of local stagnant
6 zones that can have a detrimental effect at the level of the bioprocess. The best
7 representation of fluid flow phenomena is achieved by a more complex model based on the
8 transport of momentum throughout the reactor called computational fluid dynamics (CFD).
9 CFD is based on the Navier-Stokes equations and allows the determination of a large
10 diversity of complex flow patterns, including the transition between flow regimes.
11 However, the computational difficulties associated with the related partial-differential
12 equations make it difficult to link with complex biological reaction. However, some
13 significant results have been obtained by coupling CFD with biochemical reactions (Lapin
14 A., 2006, Schmalzriedt S., 2003), but at a high computational cost. A new approach involves
15 the integration of CFD data (mainly, the orientation of the flow vectors) to build the NOZ
16 model (Bezzo, 2005). Such approach combines the power of CFD with the ease of use of the
17 NOZ models. In this work, discussion will be focused on the application of NOZ based
18 models.

19 The most critical parameter that has to be taken into account in order to simulate efficiently
20 glucose gradients generated in the SDR is the pulse frequency of the feed pump. In general,
21 different categories of behaviour can be depicted in function of the relative importance of
22 the feed pump frequency and the mixing time of the SDR or the residence time inside the
23 recycle loop:

- 24 - For a time interval between two pulses (T_{pulse}) smaller than the global mixing time of
25 the system, the mean concentrations experienced by the microorganisms are very low.
26 This is due to the fact that, between two pulses, the concentration gradient at the level
27 of the mixed part of the SDR disappears.
- 28 - For T_{pulse} approximatively equal or superior to the mixing time of the scale-down
29 reactor, concentration gradient is maintained. This concentration gradient persistence
30 leads to the increase of the mean concentration experienced by the microorganisms, as
31 well as an increase of the variance of the frequency distribution.

32 In our case, the glucose addition frequency is governed by a regulation loop involving the
33 dissolved oxygen signal, i.e. when the DO signal raise above 30% from saturation, glucose is
34 depleted and the feed pump is thus activated. On the opposite, when DO signal drops
35 below 30% from saturation, glucose is accumulating in the broth and the oxygen transfer
36 efficiency of the bioreactor is overwhelmed by the biological oxygen requirement, the feed
37 pump is thus deactivated.

38 The SDR has been modelled following a defined scheme (Fig. 11). The stirred part is
39 considered as a single perfectly mixed reactor, whereas the recycle loop exhibits a strong
40 plug flow behaviour and must then be modelled as a series of perfectly mixed reactors. The
41 hydrodynamics of the SDR has been experimentally determined (see section "material and
42 methods") and the recycle loop (in the case of the SDR with a recycle loop of $L = 12\text{m}$) has
43 been modelled as a series comprising $n = 90$ perfectly mixed reactor (backmixing flow rate
44 has been taken into account).



1
2 Fig. 11. Scheme of the hydrodynamic model showing the compartmentalization of the SDR
3 into perfectly mixed fluid zones

4 In order to illustrate the principle of compartmentalization, the following equations can be
5 considered. For the stirred part of the SDR, the evolution of concentration C (g/m^3) with
6 time t (s) on the volume of the mixed part V_m (m^3) depends on the outlet and inlet flow rates
7 q (m^3/s):

$$8 \quad V_M \cdot \frac{dC_M}{dt} = q \cdot C_{Tn} - q \cdot C_M \quad (8)$$

9 And for the recycle loop:

$$10 \quad V_{T1} \cdot \frac{dC_{T1}}{dt} = q \cdot C_M - q \cdot C_{T1} \quad (9)$$

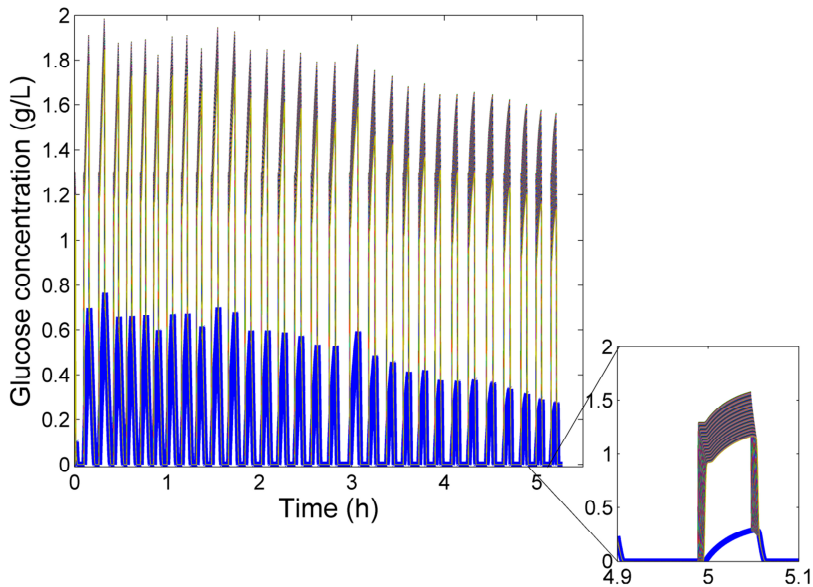
$$11 \quad V_{T2} \cdot \frac{dC_{T2}}{dt} = q \cdot C_{T1} - q \cdot C_{T2} \quad (10)$$

$$12 \quad V_{Tn} \cdot \frac{dC_{Tn}}{dt} = q \cdot C_{Tn-1} - q \cdot C_{Tn} \quad (11)$$

13 Leading to in matrix form:

$$14 \quad d \begin{bmatrix} C_M \\ C_{T1} \\ C_{T2} \\ \vdots \\ C_{Tn} \end{bmatrix} / dt = \begin{bmatrix} -q/V_M & 0 & 0 & 0 & 0 & 0 & q/V_M \\ q/V_{T1} & -q/V_{T1} & 0 & 0 & 0 & 0 & 0 \\ 0 & q/V_{T2} & -q/V_{T2} & 0 & 0 & 0 & 0 \\ 0 & 0 & 0 & \cdot & 0 & 0 & 0 \\ 0 & 0 & 0 & 0 & \vdots & 0 & 0 \\ 0 & 0 & 0 & 0 & 0 & \ddots & 0 \\ 0 & 0 & 0 & 0 & 0 & q/V_{Tn} & -q/V_{Tn} \end{bmatrix} \cdot \begin{bmatrix} C_M \\ C_{T1} \\ C_{T2} \\ \vdots \\ C_{Tn} \end{bmatrix} \quad (12)$$

1 This system of equation (equ. 12) can be resolved numerically in order to simulate, for
 2 example, the dynamics of homogenization of a substance in the SDR. In our case, we will
 3 use the model in order to simulate the glucose concentration gradient experienced by
 4 microbial cells during a fed-batch reaction performed in the SDR. In order to simulate this
 5 process, additional equations, representing the glucose addition and consumption and
 6 biomass formation must be considered. Full sample codes written in MatLab are given in
 7 annex 1 and 2. Based on these equations, the dynamics of glucose inside the SDR can be
 8 simulated (Fig. 12).
 9



10
 11 Fig. 12. Simulation of the dynamics of glucose gradient formation in SDR (in blue: glucose
 12 profile inside the stirred tank)

13 Compartmentalization of the SDR allows to take into account the formation of glucose
 14 concentration gradient. However, concentration perceived at the single cell cannot be
 15 simulated by this way. This issue will be resolved in the next section.

16 5.2 Stochastic simulation of the displacement of microbial cells along concentration 17 field

18 The displacement of microbial cells in the environment and in engineered system such as a
 19 bioreactor can be represented roughly by convection and/or diffusion-based equations,
 20 according to the nature of the conveying medium. However, one of the biggest advantages
 21 of using whole cell biosensor is their ability to detect stress at the micrometer scale. If this
 22 kind of data as to be interpreted, the environmental fluctuations have to be described at the
 23 single cell level and the random component linked with the displacement of the cell has to
 24 be taken into account. In the case of bioreactor operations, such displacement can be
 25 described by a stochastic version of the hydrodynamic presented previously. Roughly, the
 26 same equations are kept but the algorithm used to perform the simulation is quite different

1 since the stochastic component of the process has to be added to the problem. The basic
2 principle is to use the same model structure as used previously for the simulation of glucose
3 gradient by integrating a random component. The matrix M containing the exchange flow
4 rate (m³/s) of the NOZ model will be assimilated as the generator matrix Q of the stochastic
5 version of the model (Yin K.K., 2003):

$$6 \quad M = Q = \begin{bmatrix} -q_{ii} & q_{ij} & 0 & 0 & 0 & 0 \\ q_{ij} & \cdot & \cdot & 0 & 0 & 0 \\ 0 & \cdot & \cdot & \cdot & 0 & 0 \\ 0 & 0 & \cdot & \cdot & \cdot & 0 \\ 0 & 0 & 0 & \cdot & \cdot & \cdot \\ 0 & 0 & 0 & 0 & \cdot & \cdot \end{bmatrix} \quad (13)$$

7 Physically, Q contains the exchange rates (s⁻¹) between fluid zones. The main diagonal of Q
8 contains the escape rate from the ith fluid zones and is described by the vector λ:

$$9 \quad \lambda = \begin{bmatrix} q_{ii} \\ \cdot \\ \cdot \\ \cdot \\ \cdot \end{bmatrix} \quad (14)$$

10 Considering mass balance:

$$11 \quad q_{ii} = -\sum q_{ij} \quad (15)$$

12 This equation leads to the fact that the sum of each line of matrix Q (equ. 13) equal zero. This
13 property can be used to verify mass balance of the system. Value of vector λ (equ. 14) can be
14 used to compute the residence time distribution for a given fluid zone. This vector is then
15 usually called sojourn time vector. For example, in the case of a fluid zone i :

$$16 \quad P(x_i) = q_{ii} \cdot e^{-q_{ii} \cdot x_i} \quad (16)$$

17 The outlet flow rates λ_i will be used to define the occurrence of an event (i.e., in our case the
18 displacement of a microbial biosensor from a fluid zone to another). The times at which
19 events occur are determined from an exponential distribution:

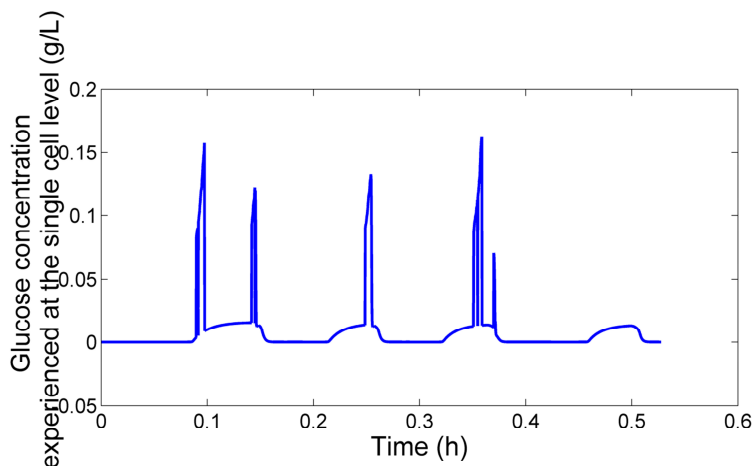
$$20 \quad T_i = -\frac{\ln(r)}{\lambda_i} \quad (17)$$

21 For which r is a random number determined from a uniform distribution on the interval [0
22 1]. When an event is determined, the displacement of the microbial biosensor, i.e. the
23 coordinates of the incoming fluid zone, is determined from the generator matrix Q (equ. 13):

$$24 \quad P = \frac{Q}{\lambda} + \begin{bmatrix} 1 & 0 & 0 & 0 & 0 & 0 \\ 0 & 1 & 0 & 0 & 0 & 0 \\ 0 & 0 & \cdot & 0 & 0 & 0 \\ 0 & 0 & 0 & \cdot & 0 & 0 \\ 0 & 0 & 0 & 0 & \cdot & 0 \\ 0 & 0 & 0 & 0 & 0 & 1 \end{bmatrix} \quad (18)$$

25 In the algorithm, event is determined by generating a random number and by comparison
26 with the probability value contained in the line of the P matrix (equ. 18) corresponding to
27 the departure fluid zone.

1 A stochastic simulation for the displacement of microbial biosensor has been performed by
2 using the SDR framework. Results of the stochastic simulation have been superimposed to
3 the deterministic simulation of the glucose gradient field in the SDR (Fig. 12), leading to the
4 glucose concentration profile experienced at the level of a single biosensor cell (Fig. 13).
5



6
7 Fig. 13. Simulation of the glucose profile experienced by a microbial biosensor if the SDR

8 At this point, it is interesting to compare GFP synthesis simulation (Fig. 4) with the
9 environmental fluctuations experienced by the biosensor in the SDR (Fig. 13).

10 **6. Enhancing the usefulness the response of GFP microbial biosensor:** 11 **measuring viability and protein leakage**

12 **6.1 Considering GFP biosensors as viability reporter**

13 In another field of study, GFP biosensors have been used in order to assess microbial
14 viability (Lehtinen, 2004). In their study, authors used unspecific whole cell microbial
15 biosensors in which GFP is constitutively expressed. When cells are exposed to stressful
16 conditions, intracellular GFP intensity is decreased following membrane damages and
17 leakage to the extracellular medium. These findings suggest that GFP can be excreted to the
18 extracellular medium following membrane permeation and/or cell lysis. Another study
19 suggests that GFP can be excreted to the extracellular medium by mechanisms other than
20 cell lysis. Indeed, *E. coli* export system can be involved in the GFP leakage (Fischer, 2008).
21 The potential impact of GFP leakage will be investigated in the next section.

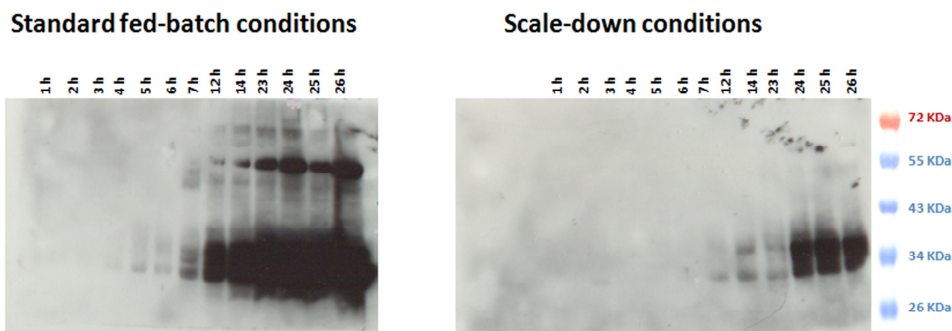
22 **6.2 Protein leakage: what is the part of the secretome that has to be considered as** 23 **indirect reporter of cell viability?**

24 During cultivations, a significant release of GFP to the extracellular medium has been
25 observed. It is known that about 30% of the proteome of Gram negative bacteria as
26 extracellular protein, this fraction being described as the secretome (Song, 2009). The
27 secretome fraction of *E. coli* comes from the leakage (and not from membrane lysis) of
28 proteins generally found in the outer membrane compartment (Nandakumar, 2006). Protein

1 leakage can be attributed to the occurrence of stress and/or changes in growth conditions.
2 There is indeed a strong correlation between growth rate, membrane stress and protein
3 leakage (Shokri, 2002, Shokri, 2004, Ling H., 2003). More recently, a series of cultivation tests
4 carried out in intensive fed-batch bioreactor validate the periplasmic origin of the secretome
5 of *E. coli* and the fact that this secretome is modulated in function of cell density and growth
6 phase (Xia, 2008). The purpose of this work is to determine if this release can be correlated to
7 the extracellular fluctuations met in the scale-down bioreactors. At this level, relationship
8 between GFP leakage and membrane permeability could also be a very interesting
9 parameter to investigate, considering the fact that cell membrane integrity based assay is
10 often used in order to assess microbial viability (Klotz, 2010). If the relationship with GFP
11 leakage can be established, this information could be potentially used to expand to use GFP
12 microbial biosensors for viability assessment. Although the proteome of *E. coli*, as well as its
13 secretome fraction has been relatively well characterized in the literature (Han, 2006), only a
14 few studies deal with the release of protein in process-related conditions. Only a single
15 study involving the characterization of the *E. coli* secretome in high cell density culture with
16 control of the main environmental variables (i.e. dissolved oxygen, glucose level, pH and
17 temperature) has been performed so far (Xia, 2008). However, this study has been
18 conducted in a lab-scale, well-mixed bioreactor. In industrial bioreactors, considering the
19 drop at the level of the mixing efficiency, microbial cells are exposed to fluctuations at the
20 level of the main environmental variables (Hewitt, 2007a, Enfors, 2001). It could be thus
21 interesting to characterize the secretome fraction affected by these fluctuations since some
22 studies suggest a strong modulation of the secretome in function of the environmental
23 conditions (Pugsley, 1998).

24 In order to get a better insight at the level of the presence of extracellular GFP, as set of SDS-
25 PAGE analysis followed by western blotting have been performed on supernatant coming
26 from the different culture conditions (Fig. 14). Western blotting of the culture supernatant
27 shows a band around 30 KDa in most of the cases. Generally this band appears more lately
28 during the culture and is more pronounced in the case of the culture performed in classical
29 bioreactor without recycle loop. This effect can be clearly observed in the case of the *csiE*
30 strain cultivated in normal mode. In this case, a strong GFP band appears after 12 and 24
31 hours of culture. In the case of the cultures operated in SDRs, the GFP band is only recorded
32 at the end of the process (24h) with a significantly lower intensity. The same relative
33 observation can be made for the *rpoS* strain. For this strain, GFP band intensity is lower in all
34 cases compared with the *csiE* strain, considering the level of expression previously
35 observed. Although the protein secretion machinery is a well known component of the *E.*
36 *coli* physiology (Pugsley, 1993), only a few studies are actually dealing with the secretion of
37 GFP to the extracellular medium. GFP has been investigated as a secretory reporter in
38 transgenic plant cells where this protein accounted for 30% of the total extracellular proteins
39 (Liu, 2001). This observation highlights the transport potential of GFP to the extracellular
40 medium. In microbial systems, GFP leakage has been considered as a marker for the
41 detection of death cells (Lowder, 2000). According to the results obtained during these
42 studies viable and viable but non culturable (VBNC) cells remained highly fluorescent,
43 whereas death cells exhibited a highly reduced fluorescence level. The drop of fluorescence
44 can be in this case attributed to the increase of the permeability of the compromised
45 membrane of death cells. The release of protein has to be attributed in this case to the
46 rupture of cell membrane under severe stress conditions (Klotz, 2010). If less severe stress
47 conditions are considered, it has been shown that protein leakage is a phenomenon

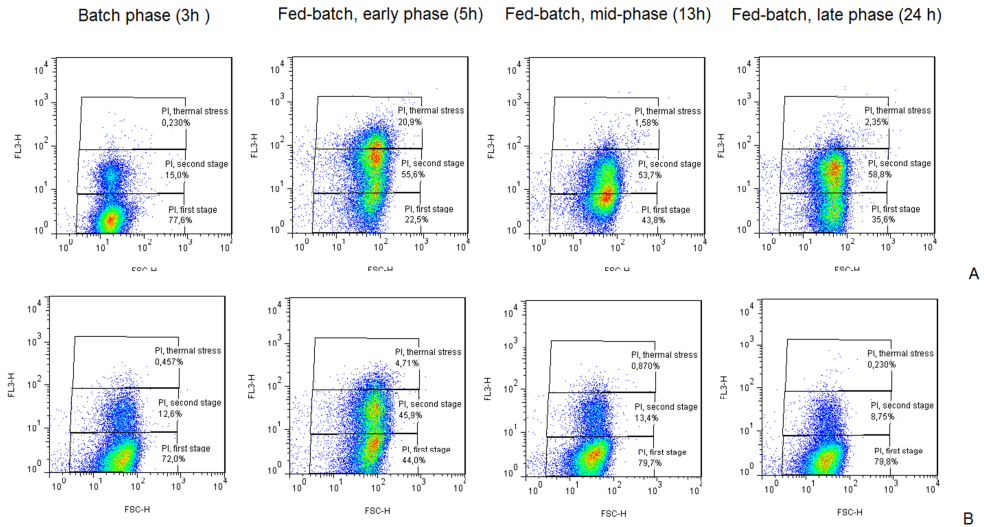
1 correlated with nutrient level, growth rate and membrane structure (Liu, 1998, Shokri, 2002).
 2 Indeed, it has been observed that a model recombinant protein (β -lactamase (Shokri, 2002))
 3 exhibited an optimal leakage at a dilution rate of 0.3 h^{-1} in chemostat. This observation has
 4 been correlated with a high membrane fluidity. This last observation makes the relation
 5 with studies involving the permeation of fluorescent product (including GFP) to assess
 6 microbial viability. At this point, it would be thus useful to determine if GFP is subjected to
 7 non specific leakage depending on the physiological state of the cell and more particularly
 8 on the state of the cellular membrane or if GFP is secreted to the extracellular medium by a
 9 specific pathway. The results obtained in this section tend to orientate our hypothesis
 10 towards a non specific leakage of GFP depending on the bioreactor operating mode. Indeed,
 11 there is no clear correlation indicating that GFP is secreted to the extracellular by a specific
 12 pathway allowing to keep a appropriate protein conformation (Fischer, 2008). This
 13 observation is supported by the fact that supernatant fluorescence levels are very low and
 14 not in accordance with the GFP concentrations recorded by western blotting.
 15



16
 17 Fig. 14. SDS-PAGE, western blotting of the supernatant for the *csiE* biosensor cultivated in
 18 standard bioreactor and in SDR

19 Microbial cells cultivated in scale-down conditions tend to exhibit a lower PI permeability
 20 than those cultivated in normal mode. This result is in accordance with previous scale-down
 21 studies involving the determination of the *E. coli* viability by multi parameter flow
 22 cytometry (Hewitt, 2000, Hewitt, 2007a). In these works, a combination of PI and BOX
 23 staining it has shown a significant drop in cell viability for cultures conducted in lab-scale
 24 bioreactors, compared with those conducted in scale-down or industrial-scale bioreactors. It
 25 has been argued that this effect can be attributed to the stress associated with glucose
 26 limitation, since cultures performed in batch and continuous mode exhibited no significant
 27 drop in cell viability (Hewitt, 1999). Another mechanism could be also the adaptation of
 28 cells cultivated in SDRs to continuously changing environment and growing at a lower
 29 growth rate (Berney, 2006). Flow cytometry profiles (Fig. 15) have been divided into three
 30 distinct subpopulation : "PI - first stage" corresponding to microbial cells stained in
 31 exponential phase ; "PI - thermal stress" corresponding to cells exposed to 60°C for 30
 32 minutes and between these two states an intermediate subpopulation depicted as "PI -
 33 second stage". It can be observed that the stressed fractions (PI-second stage and PI-thermal
 34 stress) decreased when cells are cultivated in SDRs instead of the normal mode and when
 35 residence time in the recycle loop of the SDR is increased. In general, it can be observed that

1 of GFP leakage (as shown by western blot analysis of the supernatant) is correlated with
2 higher membrane permeability as shown by PI staining tests.
3



4
5 Fig. 15. Evolution of the PI-stained population inside A : standard fed-batch bioreactor B :
6 SDR.

7 7. Conclusion and future outlook

8 Successful integration of microbial biosensors could be achieved by characterizing the
9 physico-chemical fluctuations perceived at the single cell level. Modeling procedures
10 described in this work allow the achievement this task, but some uncertainties remain at the
11 level of the dynamics of the GFP biosensor itself. It has been shown that several side
12 phenomena are interacting with the GFP synthesis, such as GFP leakage to the extracellular
13 medium. Our mathematical analysis shows that there are several similarities between the
14 biological and physical processes involved. One common feature is the stochastic
15 mechanisms associated with biosensors circulation inside the bioreactor and GFP synthesis
16 inside microbial biosensors. Both processes can be efficiently simulated by using the
17 Gillespie algorithm leading to a homogeneous mathematical formulation including the
18 biological and physical mechanisms. An important perspective of this work is the
19 elaboration of such model and its validation by dedicated experimental techniques, such as
20 flow cytometry.

21 8. Annex : MatLab .m files

22 Annex 1 : SDRdynamics.m file

23 `function dydt = SDRdynamics(t,y)`

24

25 `%% Part1 : SDR hydrodynamics`

```

1
2 % Part of the model representing the exchanges between
3 % n different fluid zones
4 % These exchanges are modelled in the matrix dF
5 n = 90; % number of fluid zones
6 V = 0.117/(n-1); % Volume of the fluid zones (recycle loop of the SDR)(in L)
7 q = 0.004; % Estimated flow rate between zones (in L/s)
8 V2 = 1; % Volume of the stirred part of the SDR (in L)
9 dF1 = diag(ones(n,1)*(-q/V));
10 dF2 = diag(ones(n-1,1)*1*(q/V),-1);
11 dF3 = diag(ones(n-1,1)*0*(q/V),1);
12 dF = dF1+dF2+dF3;
13 dF(1,1) = -q/V2;
14 dF(1,n) = q/V2;
15 dF(1,2) = 0;
16
17 %% Part2 : microbial kinetics (fed-batch mode)
18
19 %Part of the model describing consumption and addition of substrate S
20 % and its conversion into biomass X following a Monod equation
21 X = y(1:n); % Biomass concentration (in g/L)
22 S = y(n+1:2*n); % Substrate concentration (in g/L)
23
24 Sa = 400; % Substrate concentration in the feed (in g/L)
25 Yxs = 0.46; % Substrate to biomass conversion yield
26 mumax = 0.6/3600; % Maximum growth rate (in s-1)
27 Ks = 0.025; % Affinity constant for substrate S (in g/L)
28 Dmax = 0.000013; % Maximum feed flow rate (in L/s)
29
30 load oxybin3 %The vector oxybin contains a series of binary number (0 or 1)
31 %corresponding to the activation of the feed pump during
32 %a real fermentation run
33
34 rx = mumax*(S/(S+Ks))*X;
35 rs = rx./Yxs;
36 Qfeed = zeros(1,n);
37 Qfeed(2) = Dmax*Sa/V;
38 if oxybin3(round(t)+1)==0
39     Qfeed(2) = 0;
40 end
41 dXdt = rx;
42 dSdt = ((dF*S)-rs+Qfeed');
43
44 dydt = [dXdt;dSdt];
45
46

```

```

1 Annex 2 : SDRdynamicsrun.m file
2
3 n = 90;
4 y0 = zeros(1,2*n);
5 y0(1:n)=10;
6
7 options = odeset('NonNegative',2:n);
8 [t y]=ode45('SDRdynamics',0:19000,y0,odeset);
9
10 figure(1)
11 plot(t/3600,y(:,n+1:2*n))
12 xlabel('Time (h)')
13 ylabel('Glucose concentration (g/L)')
    
```

14 9. References

- 15 ASRAF-SNIR, M., GITIS, V., 2011. Tracer studies involving fluorescent-dyed
 16 microorganisms - A new method for determination of residence time in
 17 chlorination reactors. *Chemical engineering journal*, 166, 579-585.
- 18 BERNEY, M., WEILENMANN, H.U., IHSEN, J., BASSIN, C., EGLI, T., 2006. Specific
 19 growth rate determines the sensitivity of Escherichia coli to thermal, UV and solar
 20 disinfection. *Applied and environmental microbiology*, 72, 2586-2593.
- 21 BEZZO, F., MACCHIETTO, S., PANTELIDES, C.C., 2005. Computational issues in hybrid
 22 multizonal/computational fluid dynamics models. *AIChE journal*, 51, 1169-1177.
- 23 BHATTACHARYY, J., READ, D., AMOS, S., DOOLEY, S., KILLHAM, A., GRAEME, I. P.,
 24 2005. Biosensor-based diagnostics of contaminated groundwater: assessment and
 25 remediation strategy. *Environmental Pollution*, 134, 485-492.
- 26 CLEMENTSCHITSCH F., B. K. 2006. Improvement of bioprocess monitoring : development
 27 of novel concepts. *Microbial cell factories*, 5, 1-11.
- 28 CORMACK, B. P., VALDIVIA, R.H., FALKOW, R., 1996. FACS-optimized mutants of the
 29 green fluorescent protein (GFP). *Gene* 173, 33-38.
- 30 CORMACK, B. P., VALDIVIA, R.H., FALKOW, R., . 2000. *FACS optimized mutants of the*
 31 *green fluorescent protein (GFP)*.
- 32 CUI Y.Q., V. D. L. R. G. J. M., NOORMAN H.J., LUYBEN K.CH.A.M. 1996. Compartment
 33 mixing model for stirred reactors with multiple impellers. *Trans IChemE*, 74, 261-
 34 271.
- 35 DECKWER, W. D., JAHN, D., HEMPEL, D., ZENG, A.P., 2006. Systems biology approaches
 36 to bioprocess development. *Engineering in life sciences*, 6, 455-469.
- 37 DELISA, M. P., LI, J., RAO, G., WEIGAND, W.A., BENTLEY, W.E., 1999. Monitoring GFP
 38 operon fusion protein expression during high cell density cultivation of Escherichia
 39 coli using an on-line optical sensor *Biotechnology and bioengineering*, 65, 54-64.
- 40 DELVIGNE, F., DESTAIN, J., THONART, P., 2006a. A methodology for the design of scale-
 41 down bioreactors by the use of mixing and circulation stochastic models.
 42 *Biochemical engineering journal*, 28, 256-268.

- 1 DELVIGNE, F., LEJEUNE, A., DESTAIN, J., THONART, P., 2006b. Stochastic models to
2 study the impact of mixing on a fed-batch culture of *Saccharomyces cerevisiae*.
3 *Biotechnology progress*, 22, 259-269.
- 4 DIAZ, M., HERRERO, M., GARCIA, L.A., QUIROS, C., 2010. Application of flow cytometry
5 to industrial microbial bioprocesses. *Biochemical engineering journal*, 48, 385-407.
- 6 ENFORS, S. O., JAHIC, M., ROZKOV, A., XU, B., HECKER, M., JÜRGEN, B., KRÜGER, E.,
7 SCHWEDER, T., HAMER, G., O'BEIRNE, D., NOISOMMIT-RIZZI, N., REUSS, M.,
8 BOONE, L., HEWITT, C., MCFARLANE, C., NIENOW, A., KOVACS, T.,
9 TRÄGARDH, C., FUCHS, L., REVSTEDT, J., FRIBERG, P.C., HJERTAGER, B.,
10 BLOMSTEN, G., SKOGMAN, H., HJORT, S., HOEKS, F., LIN, H.Y., NEUBAUER,
11 P., VAN DER LANS, R., LUYBEN, K., VRABEL, P., MANELIUS, A. 2001.
12 Physiological responses to mixing in large scale bioreactors. *Journal of biotechnology*,
13 85, 175-185.
- 14 FINLAYSON, B. A. 2006. *Introduction to chemical engineering computing*, Wiley.
- 15 FISCHER, A. C., DELISA M.P., 2008. Laboratory evolution of fast-folding green fluorescent
16 protein using secretory pathway quality control. *Plos One*, 3, e2351.
- 17 GALBRAITH, D. W., ANDERSON, M.T., HERZENBERG, L.A., 1999. Flow cytometry
18 analysis and FACS sorting of cells based on GFP accumulation. *Methods in cell*
19 *biology*, 58, 315-341.
- 20 GARCIA, J. R., CHA, H., J., RAO, G.G., MARTEN, M.R., BENTLEY, W.E., 2009. Microbial
21 nar-GFP cell sensors reveal oxygen limitations in highly agitated and aerated
22 laboratory-scale fermentors. *Microbial cell factories*, 8, 6.
- 23 GILLESPIE D.T. 2001. Approximate accelerated stochastic simulation of chemically reacting
24 systems. *Journal of chemical physics*, 115, 1716-1733.
- 25 GUILLARD F., T. C. 1999. Modeling the performance of industrial bioreactors with a
26 dynamic microenvironmental approach : a critical review. *Chemical engineering and*
27 *technology*, 22, 187-195.
- 28 HAN L., E. S. O., HÄGGSTRÖM L. 2002. Changes in intracellular metabolite pools and
29 acetate formation in *Escherichia coli* are associated with a cell density dependent
30 metabolic switch. *Biotechnology letters*, 24, 483-488.
- 31 HAN, M. J., LEE, S.Y., 2006. The *Escherichia coli* proteome : past, present and future
32 prospects. *Microbiology and molecular biology reviews*, 70, 362-439.
- 33 HEWITT, C. J., NEBE-VON CARON, G., AXELSSON, B., MC FARLANE, C.M., NIENOW,
34 A.W., 2000. Studies related to the scale-up of high-cell-density *E. coli* fed-batch
35 fermentations using multiparameter flow cytometry : effect of a changing
36 microenvironment with respect to glucose and dissolved oxygen concentration.
37 *Biotechnology and bioengineering*, 70, 381-390.
- 38 HEWITT, C. J., NEBE-VON CARON, G., NIENOW, A.W., MC FARLANE, C.M., 1999. The
39 use of multi-parameter flow cytometry to compare the physiological response of
40 *Escherichia coli* W3110 to glucose limitation during batch, fed-batch and continuous
41 culture cultivations. *Journal of biotechnology*, 75, 251-264.
- 42 HEWITT, C. J., NIENOW, A.W., 2007a. The scale-up of microbial batch and fed-batch
43 fermentation processes. *Advances in applied microbiology*. Vol. 62.

- 1 HEWITT, C. J., ONYEAKA, H., LEWIS, G., TAYLOR, I.W., NIENOW, A.W., 2007b. A
2 Comparison of High Cell Density Fed-Batch Fermentations Involving Both Induced
3 and Non-Induced Recombinant *Escherichia coli* Under Well-Mixed Small-Scale
4 and Simulated Poorly Mixed Large-Scale Conditions. *Biotechnology and*
5 *bioengineering*, 96, 495-505.
- 6 HRISTOV H.V., M. R., LOSSEV V., VLAEV S.D. 2004. A simplified CFD for three-
7 dimensional analysis of fluid mixing, mass transfer and bioreaction in a fermenter
8 equipped with triple novel geometry impellers. *Trans IChemE*, 82, 21-34.
- 9 JOHN, G. T., KLIMANT, I., WITTMANN, C., HEINZLE, E., 2003. Integrated Optical Sensing
10 of Dissolved Oxygen in Microtiter Plates: A Novel Tool for Microbial Cultivation.
11 *Biotechnology and bioengineering*, 81, 830-836.
- 12 JONES, J. J., BRIDGES, A.M., FOSBERRY, A.P., GARDNER, S., LOWERS, R.R., NEWBY,
13 R.R., JAMES, P.J., HALL, R.M., JENKINS, O., 2004. Potential of real-time
14 measurement of GFP-fusion proteins. *Journal of biotechnology*, 109, 201-211.
- 15 KLOTZ, B., MANAS, P., MACKEY, B.M., 2010. The relationship between membrane
16 damage, release of protein and loss of viability in *Escherichia coli* exposed to high
17 hydrostatic pressure. *International journal of food microbiology*, 137, 214-220.
- 18 KOSTOV, Y., ALBANO, C.R., RAO, G., 2000. All solid-state GFP sensor. *Biotechnology and*
19 *bioengineering*, 70, 473-477.
- 20 LAPIN A., S. J., REUSS M. 2006. Modeling the dynamics of *E. coli* populations in the three-
21 dimensional turbulent field of a stirred bioreactor - A structured-segregated
22 approach. *Chemical engineering science*, 61, 4783-4797.
- 23 LARA, A. R., GALINDO, E., RAMIREZ, O.T., PALOMARES, L.A., 2006. Living with
24 heterogeneities in bioreactors - Understanding the effects of environmental
25 gradients on cells. *Molecular biotechnology*, 34, 355-381.
- 26 LEHTINEN, J., NUUTILA, J., LILIUS E.M., 2004. Green fluorescent protein - propidium
27 iodide (GFP-PI) based assay for flow cytometric measurement of bacterial viability
28 *Cytometry Part A*, 60, 165-172.
- 29 LING H., E. S. O., HÄGGSTRÖM L. 2003. *Escherichia coli* high-cell-density culture: carbon
30 mass balances and release of outer membrane components. *Bioprocess and*
31 *biosystems engineering*, 25, 205-212.
- 32 LIU, S., BUGOS, R.C., DHARMASIRI, N., SU, W.W., 2001. Green fluorescent protein as a
33 secretory reporter and a tool for process optimization in transgenic plant cell
34 cultures. *Journal of biotechnology*, 87, 1-16.
- 35 LIU, X., FERENCI, T., 1998. Regulation of porin-mediated outer membrane permeability by
36 nutrient limitation in *Escherichia coli*. *Journal of bacteriology*, 180, 3917-3922.
- 37 LOWDER, M., UNGE, A., MARAHA, N., JANSSON, J.K., SWIGGETT, J., OLIVER, J.D.,
38 2000. Effect of starvation and the viable but nonculturable state on green
39 fluorescent protein (GFP) fluorescence in GFP-tagged *Pseudomonas fluorescens*
40 A506. *Applied and environmental microbiology*, 66, 3160-3165.
- 41 MACADAMS H.H., A. A. 1997. Stochastic mechanisms in gene expression. *Proc Natl. Acad.*
42 *Sci.*, 94, 814-819.
- 43 MACHON V., J. M. 2000. Liquid homogenization in aerated multi-impeller stirred vessel.
44 *Chem. eng. technol.*, 23, 869-876.

- 1 MANN R., V. D., LOSSEV V., VLAEV S.D., ZAHRADNIK J., SEICHTER P. 1997. A network-
2 of-zones analysis of the fundamentals of gas-liquid mixing in an industrial stirred
3 bioreactor. *Récents progrès en génie des procédés*, 11, 223-230.
- 4 MARCH, J. C., RAO, G., BENTLEY, W.E., 2003. Biotechnological applications of green
5 fluorescent protein. *Applied microbiology and biotechnology*, 62, 303-315.
- 6 MARSCHALL, C., HENGGE-ARONIS, R., 1995. Regulatory characteristics and promoter
7 analysis of *csiE*, a stationary phase-inducible gene under the control of sigma S and
8 the cAMP-CRP complex in *Escherichia coli*. *Molecular microbiology*, 18, 175-184.
- 9 MAYR B., N. E., HORVAT P., MOSER A. 1993. Modelling of mixing and simulation of its
10 effect on glutamic acid fermentation. *Chem. Biochem. Eng. Q.*, 7, 31-42.
- 11 METTETAL, J. T., MUZZEY, D., PEDRAZA, J.M., OZBUDAK, E.M., VAN
12 OUDENAARDEN, A., 2006. Predicting stochastic gene expression dynamics in
13 single cells. *PNAS*, 103, 7304-7309.
- 14 MÜLLER, S., HARMS, H., BLEY, T., 2010. Origin and analysis of microbial population
15 heterogeneity in bioprocesses. *Current opinion in biotechnology*, 21, 100-113.
- 16 NANDAKUMAR, M. P., CHEUNG, A., MARTEN, M.R., 2006. Proteomic analysis of
17 extracellular proteins from *Escherichia coli* W3110. *Journal of proteome research*, 5,
18 1155-1161.
- 19 NEBE-VON-CARON G., S. P. J., HEWITT C.J., POWELL J.R., BADLEY R.A. 2000. Analysis
20 of bacterial function by multi-colour fluorescence flow cytometry and single cell
21 sorting. *Journal of microbiological methods*, 42, 97-114.
- 22 NEUBAUER, P., AHMAN, M., TÖRNKVIST, M., LARSSON, G., ENFORS, S.O., 1995.
23 Response of guanosine tetraphosphate to glucose fluctuations in fed-batch
24 cultivations of *Escherichia coli*. *Journal of biotechnology*, 43, 195-204.
- 25 NEUBAUER, P., JUNNE, S., 2010. Scale-down simulators for metabolic analysis of large-
26 scale bioprocesses. *Current opinion in biotechnology*, 21, 114-121.
- 27 NIENOW A.W. 1998. Hydrodynamics of stirred bioreactors. *Applied mechanics review*, 51, 3-
28 32.
- 29 PATKAR, A., VIJAYASANKARAN, N., URRY, D.W., SRIENC, F., 2002. Flow cytometry as a
30 useful tool for process development : rapid evaluation of expression systems.
31 *Journal of biotechnology*, 93, 217-229.
- 32 PATNAIK P.R. 2006. External, extrinsic and intrinsic noise in cellular systems : analogies
33 and implications for protein synthesis. *Biotechnology and molecular biology review*, 1,
34 121-127.
- 35 PATNAIK, P. R. 2002. Can imperfections help to improve bioreactor performance ? *Trends in*
36 *biotechnology*, 20, 135-137.
- 37 PIOCH, D., JÜRGEN, B., EVERS, S., MAURER, K.H., HECKER, M., SCHWEDER, T., 2007.
38 At-line monitoring of bioprocess-relevant marker genes. *Engineering in life sciences*,
39 7, 373-379.
- 40 PRYTZ, I., SANDEN, A.M., NYSTRÖM, T., FAREWELL, A., WAHLSTRÖM, A., FÖRBERG,
41 C., PRAGAI, Z., BARER, M., HARWOOD, C., LARSSON, G., 2003. Fed-batch
42 production of recombinant beta-galactosidase using the universal stress promoters
43 *uspA* and *uspB* in high cell density cultivations *Biotechnology and bioengineering*, 83,
44 595-603.

- 1 PUGSLEY, A. P. 1993. The complete general secretory pathway in Gram-negative bacteria.
2 *Microbiological reviews*, 57, 50-108.
- 3 PUGSLEY, A. P., FRANCETIC, O., 1998. Protein secretion in Escherichia coli K-12: dead or
4 alive? *Cell. Mol. Life Sci.*, 54, 347-352.
- 5 RANDERS-EICHHORN, L., ALBANO, C.R., SIPIOR, J., BENTLEY, W.E., RAO, G., 1997. On-
6 line green fluorescence protein sensor with LED excitation. *Biotechnology and*
7 *bioengineering*, 55, 921-926.
- 8 ROOSTALU, J., JOERS, A., LUIDALEPP, H., KALDALU, N., TENSON, T., 2008. Cell
9 division in Escherichia coli cultures monitored at single cell resolution. *BMC*
10 *microbiology*, 8, 68.
- 11 SCHMALZRIEDT S., J. M., MAUCH K., REUSS M. 2003. Integration of physiology and fluid
12 dynamics. *Advances in biochemical engineering*, 80, 19-68.
- 13 SCHWEDER, T., HECKER, M., 2004. Monitoring of stress responses. *Advances in biochemical*
14 *engineering/Biotechnology*, 89, 47-71.
- 15 SCHWEDER, T., KRÜGER, E., XU, B., JÜRGEN, B., BLOMSTEN, G., ENFORS, S.O.,
16 HECKER, M., 1999. Monitoring of genes that respond to process related stress in
17 large-scale bioprocesses. *Biotechnology and bioengineering*, 65, 151-159.
- 18 SHANER, N. C., STEINBACH, P.A., TSIEN, R.Y., 2005. A guide to choosing fluorescent
19 proteins. *Nature methods*, 2, 905-909.
- 20 SHOKRI, A., LARSSON, G., 2004. Characterisation of the Escherichia coli membrane
21 structure and function during fedbatch cultivation. *Microbial cell factories*, 3, 9.
- 22 SHOKRI, A., SANDEN, A.M., LARSSON, G., 2002. Growth rate dependent changes in
23 Escherichia coli membrane structure and protein leakage. *Applied microbiology and*
24 *biotechnology*, 58, 386-392.
- 25 SONG, C., KUMAR, A., SALEH, M., 2009. Bioinformatic comparison of bacterial secretomes.
26 *Genomics proteomics bioinformatics*, 7, 37-46.
- 27 SORENSEN, S. J., BURMOLLE, M., HANSEN, L.H., 2006. Making bio-sense of toxicity : new
28 developments in whole-cell biosensors. *Current opinion in biotechnology*, 17, 11-16.
- 29 SOUTHWARD, C. M., SURETTE, M.G., 2002. The dynamic microbe: gree fluorescent protein
30 brings bacteria to lighth. *Molecular microbiology*, 45, 1191-1196.
- 31 STORZ, G., HENGGE-ARONIS, E., 2000. *Bacterial stress response*, American Society for
32 Microbiology.
- 33 SUNDSTROM, H., WALLBERG, F., LEDUNG, E., NORRMAN, B., HEWITT, C.J., ENFORS,
34 S.O., 2004. Segregation to non-dividing cells in recombinant Escherichia coli fed-
35 batch fermentation processes. *Biotechnology letters*, 26, 1533-1539.
- 36 SWAIN P.S., E. M. B., SIGGIA E.D. 2002. Intrinsic and extrinsic contributions to stochasticity
37 in gene expression. *PNAS*, 99, 12795-12800.
- 38 TECON, R., VAN DER MEER, J.R., 2006. Information from single-cell bacterial biosensors:
39 what is it good for? *Current opinion in biotechnology*, 17, 4-10.
- 40 THATTAI M., V. O. A. 2004. Stochastic gene expression in fluctuating environments.
41 *Genetics*, 167, 523-530.
- 42 TRACY, B. P., GAIDA, S.M., PAPOUTSAKIS, E.T., 2010. Flow cytometry for bacteria :
43 enabling metabolic engineering, synthetic biology and the elucidation of complex
44 phenotypes. *Current opinion in biotechnology*, 21, 85-99.

- 1 TSIIEN R.Y. 1998. The green fluorescent protein. *Annual review in biochemistry*, 67, 509-544.
- 2 VASCONCELOS J.M.T., A. S. S., BARATA J. M. 1995. Mixing in gas-liquid contactors
3 agitated by multiple turbines. *Chemical engineering science*, 50, 2343-2354.
- 4 VRABEL P., V. D. L. R. G. J. M., VAN DER SCHOT F.N., LUYBEN K.CH.A.M., XU B.,
5 ENFORS S.O. 2001. CMA : integration of fluid dynamics and microbial kinetics in
6 modelling of large-scale fermentations. *Chemical engineering journal*, 84, 463-474.
- 7 WILES, S., WHITELEY, A.S., PHILP, J.C., BAILEY, M.J. 2003. Development of bespoke
8 bioluminescent reporters with the potential for in situ deployment within a
9 phenolic-remediating wastewater treatment system. *Journal of microbiological*
10 *methods*, 55, 667-677.
- 11 XIA, X. X., HAN, M.J., LEE S.Y., YOO, J.S., 2008. Comparison of the extracellular proteomes
12 of Escherichia coli B and K-12 strains during high cell density cultivation.
13 *Proteomics*, 8, 2089-2103.
- 14 XU, B., JAHIC, M., BLOMSTEN, G., ENFORS, S.O., 1999. Glucose overflow metabolism and
15 mixed-acid fermentation in aerobic large-scale fed-batch processes with Escherichia
16 coli. *Applied microbiology and biotechnology*, 51, 564-571.
- 17 YIN K.K., Y. H., DAOUTIDIS P., YIN G.G. 2003. Simulation of population dynamics using
18 continuous-time finite-state Markov chains. *Computer and chemical engineering*, 27,
19 235-249.
- 20 ZAHRADNIK J., M. R., FIALOVA M., VLAEV D., VLAEV S.D., LOSSEV V., SEICHTER P.
21 2001. A network-of-zones analysis of mixing and mass transfer in three industrial
22 bioreactors. *Chemical engineering science*, 56, 485-492.
- 23 ZASLAVER, A., BREN, A., RONEN, M., ITZKOVITZ, S., KIKOIN, I., SHAVIT, S.,
24 LIEBERMEISTER, W., SURETTE, M.G., ALON, U., 2006. A comprehensive library
25 of fluorescent transcriptional reporters for Escherichia coli. *Nature methods*, 3, 623-
26 628.
- 27 ZHANG, Q., ANDERSEN, M.E., CONOLLY, R.B., 2006. Binary gene induction and protein
28 expression in individual cells. *Theoretical biology and medical modelling*, 3, 18.